Non-linear stochastic inversion of regional Bouguer anomalies by means of Particle Swarm Optimization: Application to the Zagros Mountains

Ali Jamasb[1] and Seyed-Hani Motavalli-Anbaran[2*]

[1] *M. Sc. Student, Institute of Geophysics, University of Tehran, Tehran, Iran*
[2] *Assistant Professor, Institute of Geophysics, University of Tehran, Tehran, Iran*

(Received: 15 September 2016, Accepted: 21 November 2016)

Abstract

Estimating the lateral depth variations of the Earth's crust from gravity data is a non-linear ill-posed problem. The ill-posedness of the problem is due to the presence of noise in the data, and also the non-uniqueness of the problem. Particle Swarm Optimization (PSO) is a stochastic population-based optimizer, originally inspired by the social behavior of fish schools and bird flocks. PSO is a global search method, meaning that it has the ability to escape local minima. In addition, PSO is an iterative method, wherein an initial solution is chosen randomly and then improved iteratively until the algorithm finds a solution close enough to the global minimum. Herein, the inverse problem of estimating the thickness of the crust from gravity anomalies is formulated as a single objective optimization problem and is solved by PSO. The method is first tested on a realistic synthetic crustal model both with and without the presence of white Gaussian noise (WGN). Then it is applied to the gravity data from EIGEN-6c4, the latest combined global gravity model, in order to find the base of the crust in the Zagros Mountains (Iran) and compare the results with those of other geophysical methods. The assumed crustal model is one with a linear density gradient in which the densities at both the surface and the base of the crust are fixed. Results agree well with the previously published works including both seismic and potential field studies.

Keywords: gravity data, particle swarm optimization (PSO), Zagros Mountains

[*]Corresponding author: motavalli@ut.ac.ir

1 Introduction

The nonlinear inverse problem of estimating the depth of a layer from gravity data is one of the oldest geophysical inverse problems (e.g. Bott, 1960; Bott, 1965). For instance, gravity methods have been vastly used to estimate the base of sedimentary basins (Silva et al., 2014 and references therein). Due to the non-linear relationship of gravity and depth, the inverse problem of inverting the gravity data for depth is nonlinear. Classically, deterministic local searches, such as Levenberg–Marquardt (LM) or Gauss–Newton (GN), have been employed to solve the non-linear inverse problem (e.g. Zeyen and Pous, 1993; Čuma et al., 2012). Although, these local searches converge very fast, they have a number of disadvantages mostly due to the ill-posedness of the nonlinear gravity inverse problem. On the one hand, these methods begin their search at an arbitrary initial model and then improve it iteratively. As a result, the solutions of these methods highly correlate with the quality of the initial model (also called initial guess). This could be highly problematic since these methods are based on local search algorithms, hence if the proper initial model is not chosen, they could easily get stuck in local minima caused by non-uniqueness. In addition, the improvement of the solution at each iteration is done by calculating the first derivatives of the objective function with respect to model parameters. This could result in extra calculations since it might not always be possible to calculate the derivatives analytically. On the other hand, since the data contain noise, it is not only impossible to find an exact solution for the inverse problem, but also such solution is not desired because an exact solution would be one that has been found by inverting the noise contained within the data.

Globally available potential field data offer valuable information about the Earth's interior especially at crustal scales (e.g. Aitken et al., 2013). Gravity method is a suitable alternative for seismic methods in regions of sparse data coverage (Grad and Tiira, 2012). In addition to low data coverage, various factors such as crustal anisotropy, different model parameterization or different inversion techniques could also change modelling results of different seismic methods including refraction and reflection methods and receiver function (RF) analyses (Grad and Tiira, 2012; Mutlu and Karabulut, 2011). As a stochastic global method, the Particle Swarm Optimization (PSO) is an excellent minimizer for the non-linear gravity inverse problem, since its solution does not rely on an initial guess. Moreover, PSO performs fairly well without the use of explicit a priori information, and hence, when used with satellite gravity data, could be a strong method in regions with low seismic data coverage.

Recently, approximation algorithms or metaheuristics have been used as alternatives to the LM and GN methods. Metaheuristics are designed to solve hard optimization problems which are those problems for which finding an exact solution is not possible in limited times (Gonzalez, 2007; Sen and Stoffa, 2013). Evolutionary Algorithms (EAs), Simulated Annealing (SA), and Swarm Intelligence Algorithms (SIAs) are among well-known metaheuristics of which EAs and SIAs are referred to as population-based algorithms. EAs are inspired by Darwinian Evolutionary theory (Gould, 2002) wherein a population of "genes" (possible solutions to the problem) compete to survive. Genetic algorithm and evolution strategies are among the most well-known EAs (Bäck and Schwefel, 1993; Bäck, 1996). Similarly, in SIAs a

population is in search for the best solution with one important difference. In SIAs, instead of competing, the population collaborates to find the best solution. Ant colony optimization (Dorigo et al., 1996) and PSO (Eberhart and Kennedy, 1995) are the two most well-known families of SIAs.

Ant colony optimization has been recently used to solve the inverse problem of inverting the potential field data (Liu et al., 2014). The PSO has also been used in a number of geophysical inverse problems including Vertical Electric Sounding (VES) and magnetotelluric (Shaw and Srivastava, 2007), self-potential (Monteiro Santos, 2010), and a 2D analytical signal of magnetic anomalies (Srivastava and Agarwal, 2010). However, up to now, the PSO has not been used in gravity studies at crustal scales.

2 Particle Swarm Optimization

The PSO is a stochastic global search method which belongs to the family of SIAs (Kennedy et al., 2001). Inspired by the social behavior of real swarms, the PSO performs its search for the global minimum by means of a set of particles within the bounds of a pre-defined search space (Eberhart and Kennedy, 1995). The expression "social behavior of real swarms" refers to the way by which the members of the swarm collaborate in time with the aim of finding food. As the time goes by, those possible places where food might exist are memorized by those individuals who have found them. Then, other members are notified through communication and change their direction towards those places. This description is in fact quite simplified and probably inaccurate. Formally, in biology, this process is called self-organization (Garnier et al., 2007) which is described as a set of dynamic mechanisms taking place within the lower levels by which the structures at global levels are controlled without any explicit coding on individuals. Self-organization is the primary difference between swarm intelligence algorithms and evolutionary algorithms. In the latter, the explicit coding on the individuals is done via a set of operators such as mutation and/or selection (e.g. see Angeline, 1998). In PSO, each particle is characterized by its position in the search space. That position is in fact a potential solution to the optimization problem. In the beginning of the search, the positions of the particles are set randomly within the bounds of the search space.

In order to be able to present the mathematical formulas of PSO, a few terms have to be defined first. In doing this, without any loss of generality, a one-dimensional minimization problem is assumed. The search space is defined as an arbitrary interval such as $[X_0, X_1] \subset \mathcal{R}$ in which the global minimum of *f(x)* is located. The global best position (G_{best}) until iteration K (that is until $t=K$) amongst the swarm is defined as:

$$x = G_{best} \; if \; f(x) < f\left(x_i^k\right) for \; \forall x_i^k \; \epsilon [x_0, x_1] \,, \quad \text{(Definition 1)}$$

where $i = 1, 2, \dots, N$ and $k = 1, 2, \dots K$ with N being the swarm size (i.e. the number of particles in the swarm). It is apparent from Def. 1 that at any time during the PSO search, there is only one global best position which has yielded the best result (i.e. the lowest obtained value for the objective function) until that time. Similarly, a personal best position (P_{best}) is also defined for each particle in the swarm as:

$$x = P_{best} \; if \; f(x) < f(x^k) \; for \; \forall x^k \; \epsilon [x_0, x_1] \,. \quad \text{(Definition 2)}$$

In addition to position, each particle also has a velocity at each time which is the distance that a particle should travel

for the next iteration (i.e. in 1 second) to get to its next position. The velocity update equation of each particle is given as (Shi and Eberhart, 1998):

$$v_i^{k+1} = \omega \,.\, v_i^k + c_1 \,.\, r_1 \left({G_{best}}^k - x_i^k\right) + c_2 \,.\, r_2 \left({P_{i,best}}^k - x_i^k\right). \quad (1)$$

And hence, the update equation for the position of the particles would become (Shi and Eberhart, 1998):

$$x_i^{k+1} = x_i^k + v_i^{k+1}\,, \quad (2)$$

where x_i^k and v_i^k are the position and velocity of particle i at iteration k respectively, ω is called the inertia weight, k is the current iteration, $i=1,2,\ldots,N$ indicates the ith particle with N being the swarm size, $r_1 \,\&\, r_2 \in (0 \ldots 1)$ are random numbers chosen uniformly, and finally $c_1 \,\&\, c_1$ are called social and cognitive coefficients respectively (also called acceleration coefficients).

In eq. (1), the subtractions are probably best interpreted in terms of calculating a distance between a particle current position (x_i^k) and the global (the second term in the right hand side of eq. (1)) or personal (the third term) best positions. These distances would indicate how far a particle is actually located from these best positions. If these distances are small, then the velocity would be small, meaning that the particle is probably somewhere near the global best solution. However, the random numbers, along with c_1 and c_2 give weights to these distances. The first term on the right-hand side of eq. (1), which is the velocity from the last iteration, also makes sure that the direction of a particle toward its next position is also based on previous global and personal best positions which help to escape local minima.

3 Inversion

Solving a non-linear inverse problem is comprised of two stages: formulating an objective function by defining a forward problem, and minimizing that objective function with respect to the desired model parameters by imposing necessary constraints. In the first stage, the continuous physical space has to be discretized since the data are usually discrete. In the second stage, a minimizer is used to find the best solution for the problem, i.e. one that minimizes the objective function best. The objective function consists of a data misfit term in addition to smoothing terms. The data misfit (MF) is the difference between the data calculated by candidate solutions and the actual observed values. From a mathematical point of view, the general forward problem could be defined as:

$$\vec{d} = f(\vec{m})\,, \quad (3)$$

where $\vec{d}$ is the vector containing the data (knowns), $\vec{m}$ is the vector of model parameters (unknowns), and f is the non-linear physical relationship between $\vec{d}$ and $\vec{m}$. In the case of gravity (g) and depth (z), eq. (1) could be rewritten as:

$$\vec{g} = f(\vec{z})\,, \quad (4)$$

where f depends on the way that the discretization of the underground space is carried out. In fact, the discretization could be performed in various schemes based on the needs of the problem. The discretization divides the physical underground space into a set of compartments where each one is associated with a model parameter. On the one hand, the number of the compartments determines the number of the required calculations and consequently the time needed for the inversion. On the

other hand, the number of the compartments is actually the number of the model parameters, hence it should be set by some care in order to avoid the inverse problem becoming under-determined, i.e. when the number of the unknowns is greater than the number of the knowns, which causes ill-posedness (Zhdanov, 2002). In addition, the discretization also has to consider realistic situations. For instance, in inverting Bouguer anomalies at crustal scales, assuming a constant density for the crust is rather unrealistic due to both lateral and vertical density variations within the crust. As a result, one has to take into account these considerations. Although there are a number of analytical relations for the vertical density variations of the crust, there is not an established relation for the lateral density variations of the crust since they have rather anomalous sources. For instance, in sedimentary basins, an exponential or quadratic relation is usually assumed for the vertical density variations (e.g. Rao et al., 1995; Rao, 1990; Cordell, 1973). However, at crustal scales a linear density gradient is more customary (e.g. Motavalli-Anbaran et al., 2016; Afonso et al., 2008). It has been shown that for the same average crustal densities, the gravity effects of a linear gradient crustal model and an exponential one do not vary greatly (Motavalli-Anbaran et al., 2013).

Hereby the underground space is divided into a set of right rectangular prisms with a linear density gradient. Each data point is associated with one prism, and hence the number of model parameters and the data are equal. Gallardo-Delgado et al. (2003) give the analytical formula for the vertical gravitational attraction of a right rectangular prism in the Cartesian coordinates with linear density gradient as:

$$
\begin{aligned}
g = G\rho_0 \,|||\, & x\ln(y+r) + y\ln(x+r) \\
& - z\arctan\left(\frac{xy}{zr}\right) \Big|_{x1}^{x2}\Big|_{y1}^{y2}\Big|_{z1}^{z2} + G\gamma \,|||\, \\
& - xy\ln(r+z) - \frac{z^2}{2}\arctan\left(\frac{xy}{zr}\right) \\
& + \frac{x^2}{2}\arctan\left(\frac{yz}{xr}\right) + \frac{y^2}{2}\arctan\left(\frac{xz}{yr}\right) \Big|_{x1}^{x2}\Big|_{y1}^{y2}\Big|_{z1}^{z2}
\end{aligned} \tag{5}
$$

$$\rho(z) = \rho_0 + \gamma z$$

$$r = \sqrt{x^2 + y^2 + z^2}$$

G = Universal gravitational constant (6.6726 × 10^{-11}),

where ρ_0 is the density at the top and γ is the rate with which the density increases with depth. Eq. (5) calculates the gravity effects of one right rectangular prism on a single observation point. The model parameters in the inversion are therefore the thicknesses of the prisms. Assuming that the observed Bouguer anomalies are solely comprised of the contributions by the considered area, each observed Bouguer anomaly would be the sum of the gravity effects of all prisms at that observation point. Thereby, the data misfit term in the objective function should be minimized in a least-squares sense in order to find the global minimum, i.e. the true set of the thicknesses of the prisms. The final objective function could be written as:

$$
\begin{aligned}
\varphi(z) = & \sum_{i=1}^{N}\left(\frac{g_i^{obs} - \sum_{j=1}^{M} g_j^{calc}}{\sigma_g^i}\right)^2 + \\
& \mu_z \sum_{j=1}^{M-1}\left(\left|z_{j+1} - z_j\right|\right)^2 + \\
& \sum_{j=1}^{M}\left(\lambda_j \left|\frac{z_j - z_j^{apr}}{\sigma_z^j}\right|\right).
\end{aligned} \tag{6}
$$

Eq. (6) is non-linear in which the first term in the right hand side is the data misfits. The second term is the smoothing term, in which μ, called the stabilizing parameter (km^{-2}), controls the importance of the smoothing term. The last term is for explicit a priori information in which λ_j is called the damping factor and is

nonzero for points where a priori information are used. Also σ_j is the corresponding uncertainty of the independent a priori information which incorporates a sense of reliability of the a priori information used into the calculations. In eq. (6), $\varphi(z)$ is dimensionless and is the final objective function that has to be minimized.

Instead of the usual matrix forms which are customary in geophysical inverse problems, Eq. (6) is expressed in a term by term manner since using PSO for finding the best set of $\mathbf{z}$ which minimizes $\varphi(\boldsymbol{z})$ involves neither calculating a Jacobian matrix nor any matrix inversions.

4 Synthetic tests

In order to test the ability of PSO in solving the non-linear problem of inverting Bouguer anomalies for depth, a realistic 2D synthetic crustal model with an average thickness of ~30 km was defined. The length of the defined profile is 600 km along which there are two crustal thickenings where the Moho reaches depths of 42 km and 50 km. By assuming a linear vertical density gradient, the "observed" data are calculated by means of eq. (5) on equally spaced observation points (Figure 1).

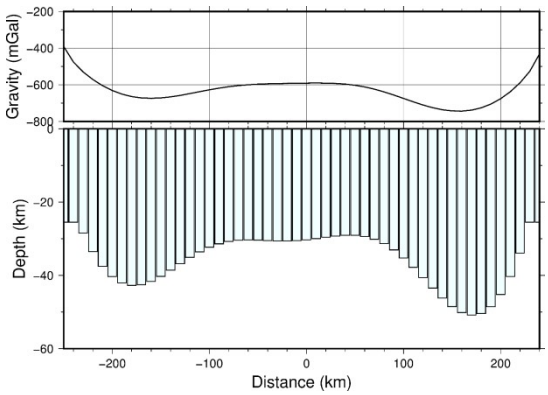

Figure 1. The discretization of the underground space is carried out via a set of right rectangular prisms with linear density gradient.

The synthetic tests are performed both with and without the presence of white Gaussian noise. Since PSO is a stochastic method, its results are not the same upon repetition, or in other words, in two repetitions of PSO, the movements of the particles are not along the same path in the search space due to the use of random numbers in eq. (1), and therefore the results are not necessarily the same. Hence, it is necessary to repeat the search for an optimum number of times before selecting the final solution. Hereby, based on our experiments, the minimization is repeated 30 times for each case. Figure 2 shows the results for the data without noise. The relative error of the calculated solution is shown in the bottom panel. With the exception of border points, the majority of the estimated depths have a relative error below 2%. The high relative error of the estimated depths at the two ends of the profile may be due to the lack of required information at those observation points. This issue is even more problematic in the case of real data where the physical space with a continuous nature is discretized in the form of a profile. Although the modeling procedure assumes that the observed Bouguer anomaly is completely caused by the region enclosed in the profile (e.g. the 2D cross section in Figure 1), in reality this value is partly made by contributions of the outside area. This issue is addressed in the next section.

The results of the tests on synthetic data, contaminated with 3% white Gaussian noise (WGN), is shown in Figure 3. In using PSO as a minimizer, the uncertainties of the solutions cannot be calculated directly. In order to calculate the uncertainty of the depths, all the solutions throughout the 30 repetitions of the runs are saved, where for each solution the corresponding WGN is regenerated independently, and the standard deviation of all 30 solutions are calculated and stored as a vector $\boldsymbol{\sigma}$.

Hence, the length of **σ** is equal to the number of the defined blocks (i.e. the number of model parameters). In the bottom panel of Figure 3, the vector 2**σ** is presented as the uncertainty of the solutions. In addition to the aforementioned differences between PSO solutions due to its stochastic nature, in working with real data this scheme for calculating uncertainty also yields a sense of reliability of the method upon slight changes in the initial parameters of the inversion such as the assumed densities at the top and bottom, the maximum number of PSO iterations, the number of particles in the swarm (i.e. swarm size), etc. (see also Motavalli-Anbaran et al., 2013; 2016 for a discussion on calculating the uncertainty).

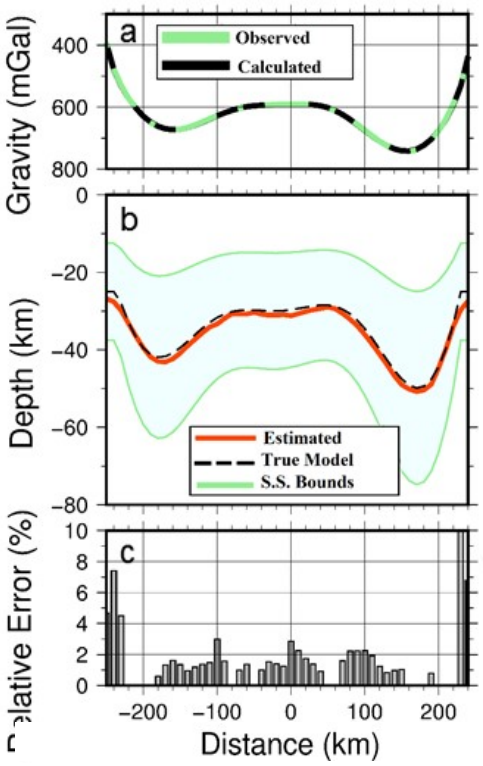

Figure 2. (a) The calculated and observed Bouguer anomalies. (b) Reconstructed and true models. (c) The relative error of the reconstructed model.

Based on the results presented in Figures 2 and 3, it can be concluded that PSO has been successful in solving the non-linear inverse problem of inverting Bouguer anomalies for the depth of Moho boundary. Finally, Table 1 shows the PSO parameters used for the inversion.

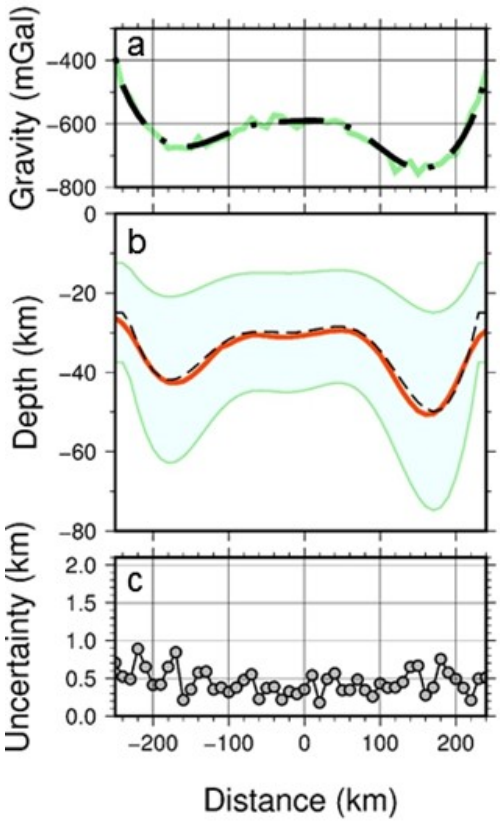

Figure 3. (a) The calculated and observed (with 3% white Gaussian noise) Bouguer anomalies. (b) Reconstructed and true models. (c) The relative error of the reconstructed model. The legend is the same as in Figure 2.

Table 1. The parameters used for the synthetic tests. The acceptable interval for the smoothing factor is found by trial and error.

C_1	C_2	Swarm Size	Max Iteration	Smoothing factor
1.5	2	250	100-150	0.00075 to 0.01

5 Real data

Although the synthetic tests in section 4 assessed the ability of PSO in solving the non-linear gravity inverse problem, its

performance has to be compared with other geophysical methods. For this, in this section, we use real data to find the lateral variation in the depth to the base of crust along a profile and compare our results with the results of seismic tomography and integrated geophysical modeling.

The Zagros Mountains (Figure 4) are formed by opening and closure of the Neo-Tethys oceanic realm (Alavi, 1994). The tectonic evolution and seismo-tectonics of Zagros have been extensively studied in the last few decades (e.g. Berberian, 1995; Al-Lazki et al., 2004; Hatzfeld et al., 2003; Hafkenscheid et al., 2006; Al-Lazki et al., 2014; Dewey et al., 1986). The Zagros is comprised of three almost parallel tectonic settings which are extended from northwest to southeast, namely Zagros Fold and Thrust Belt (ZFTB), Sanandaj–Sirjan Zone (SSZ), and Urmia–Dokhtar Magmatic Assemblage (UDMA) (Alavi, 1994). The highest topography is in the Main Zagros Thrust (MZT), which marks the continental collision of Eurasian–Arabian plates (Barazangi et al., 2006 and references therein). The lithospheric structures of Zagros have been studied using various geophysical methods (e.g. Molinaro et al., 2005; Manaman et al., 2011; Al-Lazki et al., 2014; Motavalli-Anbaran et al., 2011). In particular, the crustal structure of Zagros has been the subject of various studies for a long time. Using the data from a 620 km long array. Paul et al. (2006) found an average crustal thickness of ~50 km in Zagros with a relatively short wavelength thickening beneath the SSZ where Moho reaches the depth of 70 km. Later, Manaman and Shomali (2010) investigated the upper mantle structure and Moho depth variations along the same profile and found an average ~45 km thickness for the crust with a thickening beneath ZFTB and SSZ. Motavalli-Anbaran et al. (2011) integrated gravity, geoid, and topography data in a forward modeling procedure along three SW-NE profiles, amongst which, the first half of profile III coincides with the ones from aforementioned works. Their results revealed that, on average, the base of the crust lies at a depth of ~55 km beneath Zagros. However, contrary to the reports of Paul et al. (2006), Motavalli-Anbaran et al. (2011) found a much smoother thickening beneath the MZT where the topography is the highest. Finally, they concluded that, based on the fits of both gravity and geoid, the crustal model of Manaman and Shomali (2010) has a better chance to be closer to reality.

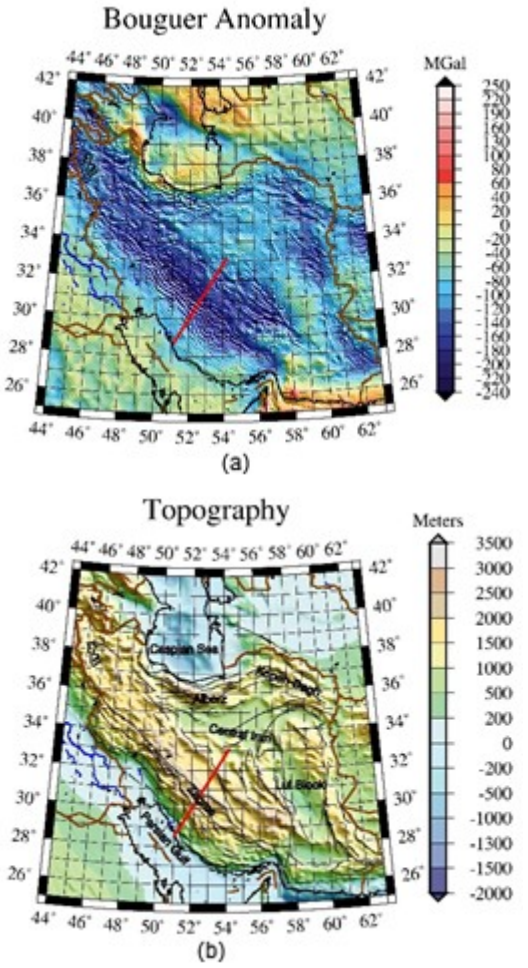

Figure 4. (a) Topography of Iran. (b) The map of Bouguer anomalies for Iran. The red line depicts the profile used for the Zagros

Herein, PSO is used to estimate the depth to the base of crust in Zagros mountains (Iran) along the same profile as in Paul et al. (2006). The gravity data (Figure 5) are extracted from EIGEN 6c4, a combined high-resolution global gravity model including GOCE data up to degree and order 2190 (Förste et al., 2014). Prior to the calculations, the data were stacked over a total 1-degree envelope, and then filtered using a 150 km low-pass Gaussian filter to eliminate shallow and short wavelength effects (see Gómez-Ortiz et al. (2011) for a discussion on choosing the cutoff wavelength). In addition, the gravity signature of density variations deep within the upper-mantle was also calculated from EGM2008 (Pavlis et al., 2012) by considering degrees up to 30 (suggested by Corchete et al., 2010) and subtracted from the regional Bouguer anomalies. Usually, this last step is not necessary due to the fast decay of gravity with distance (i.e. $g \propto \frac{1}{r^2}$) as is suggested by Motavalli-Anbaran et al. (2013). However, recent studies have revealed a lithospheric thinning beneath the MZT via modeling of potential field data where the base of lithosphere reaches a depth of ~170 km (Molinaro et al., 2005), which is well apparent in the Bouguer data.

For calculating the forward problem, the temperature at the base of the crust was assumed to be 800 °C which results in a density contrast of -317 kg/m^3 between the lower crust and upper mantle based on the values suggested by Motavalli-Anbaran et al. (2011). The density at the surface is assumed to be -467 kg/m^3 with a linear density gradient crustal model. In order to overcome the aforementioned difficulties with the observation points at the two ends of the profile (see section 4), two strategies were adopted. First, the actual profile, on which the calculations are carried out, was extended in both directions. Second, the last block at each end was also artificially extended as suggested by Afonso et al. (2008). However, the presented results are only for a 400 km long profile with the origin at the MZT.

The parameters used in the inversion are presented in Table 2. The calculations were repeated 30 times, and the results are presented in Figure 6. The average calculated depth to the base of the crust is ~ 54 ± 3 km. Results also show a thickening beneath the MZT where the topography is the highest where Moho depth reaches ~ 60 km. As can be seen, the solutions agree with the ones from Manaman and Shomali (2010) and Motavalli-Anbaran et al., 2011. However, the estimated Moho depth in the easternmost part of the profile is greater than the previous works. This is most probably due to an over-estimation of the density contrast between the crust and the lithosphere mantle since the same density contrast is used along the profile in the calculations. The results of recent Pn tomography (Al-Lazki et al., 2014),

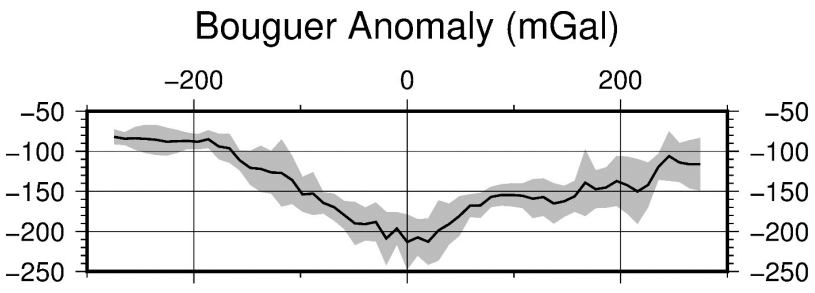

Figure 5. The stacked Bouguer anomaly along the selected profile. The origin is located on MZT. See Figure 6 for the filtered data.

Table 2. The parameters used for the inversion of real data. The densities at both the surface and the bottom of the crust were varied within a 50 kg/m^3 interval.

C_1	C_2	Swarm Size	Max Iteration	Smoothing factor	$\Delta\boldsymbol{\rho_{surface}}$ (kg/m^3)	$\Delta\boldsymbol{\rho_{bottom}}$ (kg/m^3)
1.5	2	250	100-150	0.0075 to 0.01	[-433 to -467]	[-283 to -317]

higher S velocity (Manaman et al., 2011), and higher vertical integral of the lithospheric strength (Motavalli-Anbaran et al., 2011) also suggest that the Arabian foreland (south of MZT) may have a higher density than the Eurasia part which would result in a smaller density contrast.

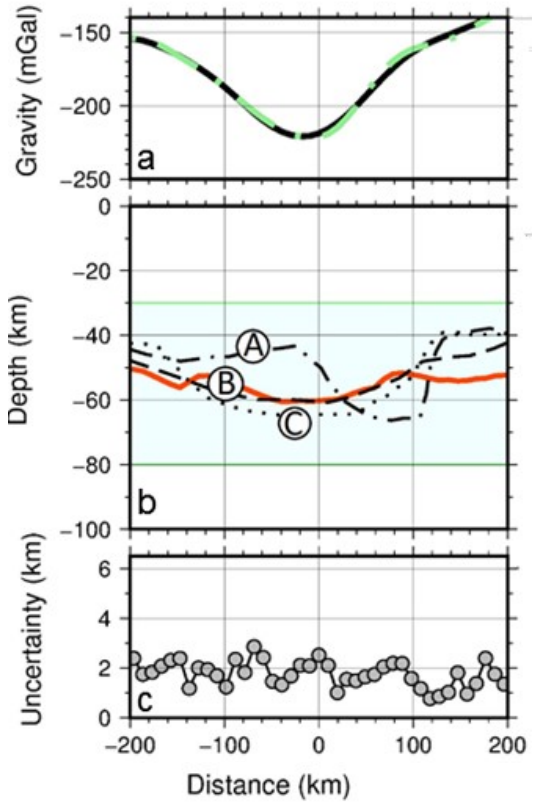

Figure 6. The inversion results for the Zagros Profile. (a) Calculated and observed Bouguer anomalies (b) Reconstructed and the results of previous works. (c) The uncertainty of the reconstructed model. The legend is the same as in Figure 2. A: crustal model by Paul et al. (2006); B: Motavalli-Anbaran et al. (2011); C: Manaman and Shomali (2010).

The lower panel in Figure 6 shows the uncertainty of the solutions, which is on average ~3 km. It should be noted that gravity is generally a low-resolution method, and a 4~5 km uncertainty is customary (Grad and Tiira, 2009).
Finally, it is noteworthy that the constraining of the solutions was carried out without the use of any explicit a priori information (in eq. (6), $\lambda = 0$ for all of the blocks). Also, the smoothing factor in eq. (6) was found by trial and error. Based on the presented results, PSO has been able to give satisfactory solutions.

6 Conclusions

We used PSO to solve the non-linear problem of inverting gravity data for depths to the base of the crust in the Zagros Mountains. Our results are in good agreement with results of previous seismic works. Thereby, metaheuristics and PSO in particular seem to be reliable alternatives for deterministic local search methods, especially in regions with sparse seismic data coverage.

Acknowledgment

The figures presented have been prepared using the Generic Mapping Tools (Wessel et al., 2013).

References

Afonso, J. C., Fernández, M., Ranalli, G., Griffin, W., and Connolly, J., 2008, Integrated geophysical–petrological modeling of the lithosphere and sublithospheric upper mantle: Methodology and applications: Geochemistry, Geophysics, Geosystems, **9** (5), 1–36.

Aitken, A. R. A., Salmon, M. L., and Kennett, B. L. N., 2013, Australia's Moho: A test of the usefulness of gravity modelling for the determination of Moho depth: Tectonophysics, **609**, 468–479.

Al-Lazki, A. I., Al-Damegh, K. S., El-Hadidy, S. Y., Ghods, A., and Tatar, M., 2014, Pn-velocity structure beneath Arabia–Eurasia Zagros collision and Makran subduction zones: Geological Society, London, Special Publications, **392**, 45–60.

Al-Lazki, A. I., Sandvol, E., Seber, D., Barazangi, M., Turkelli, N., and Mohamad, R., 2004, Pn tomographic imaging of mantle lid velocity and anisotropy at the junction of the Arabian, Eurasian and African plates: Geophys. J. Int., **158**, 1024–1040.

Alavi, M., 1994, Tectonics of the Zagros orogenic belt of Iran: new data and interpretations: Tectonophysics, **229**, 211–238.

Angeline, P. J., 1998, Using selection to improve particle swarm optimization: paper presented at Proceedings of IEEE International Conference on Evolutionary Computation, Citeseer.

Bäck, T., 1996, Evolutionary Algorithms in Theory and Practice: Evolution Strategies, Evolutionary Programming, Genetic Algorithms: Oxford University Press, 328 pp.

Bäck, T., and Schwefel, H.-P., 1993, An overview of evolutionary algorithms for parameter optimization: Evolutionary Computation, 1, 1–23.

Barazangi, M., Sandvol, E., and Seber, D., 2006, Structure and tectonic evolution of the Anatolian plateau in eastern Turkey: Geological Society of America Special Papers, **409**, 463–473.

Berberian, M., 1995, Master "blind" thrust faults hidden under the Zagros folds: active basement tectonics and surface morphotectonics: Tectonophysics, **241**, 193–224.

Bott, M., 1960, The use of rapid digital computing methods for direct gravity interpretation of sedimentary basins: Geophys. J. Int., **3**, 63–67.

Bott, M., 1965, The upper mantle beneath Iceland: Geophys. J. Int., **9**, 275–277.

Corchete, V., Chourak, M., and Khattach, D., 2010, A methodology for filtering and inversion of gravity data: an example of application to the determination of the Moho undulation in Morocco: Engineering, **2**, 149–159.

Cordell, L., 1973, Gravity analysis using an exponential density-depth function—San Jacinto Graben, California: Geophysics, **38**, 684–690.

Čuma, M., Wilson, G. A., and Zhdanov, M. S., 2012, Large-scale 3D inversion of potential field data: Geophys. Prospect., **60**, 1186–1199.

Dewey, J., Hempton, M., Kidd, W., Saroglu, F. T., and Şengör, A., 1986, Shortening of continental lithosphere: the neotectonics of Eastern Anatolia—a young collision zone: Geological Society, London, Special Publications, **19**, 1–36.

Dorigo, M., Maniezzo, V., and Colorni, A., 1996, Ant system: optimization by a colony of cooperating agents: IEEE Transactions on Systems, Man, and Cybernetics, Part B: Cybernetics, **26**, 29–41.

Eberhart, R. C., and Kennedy, J., 1995, A new optimizer using particle swarm theory: Proceedings of the 6th International Symposium on Micro Machine and Human Science, New York, NY.

Förste, C., Bruinsma, S., Abrikosov, O., Flechtner, F., Marty, J.-C., Lemoine, J.-M., Dahle, C., Neumayer, H., Barthelmes, F., and König, R., 2014, EIGEN-6C4 The latest combined global gravity field model including GOCE data up to degree and order 1949 of GFZ Potsdam and GRGS Toulouse: EGU General Assembly Conference Abstracts.

Gallardo-Delgado, L. A., Pérez-Flores, M. A., and Gómez-Treviño, E., 2003, A versatile algorithm for joint 3D inversion of gravity and magnetic data: Geophysics, **68**, 949–959.

Garnier, S., Gautrais, J., and Theraulaz, G., 2007, The biological principles of swarm intelligence: Swarm Intelligence, **1**, 3–31.

Gómez-Ortiz, D., Agarwal, B., Tejero, R., and Ruiz, J., 2011, Crustal structure from gravity signatures in the Iberian Peninsula: Geological Society of America Bulletin, **123**, 1247–1257.

Gonzalez, T. F., 2007, Handbook of Approximation Algorithms and Metaheuristics: CRC Press, 1432 pp.

Gould, S. J., 2002, The Structure of Evolutionary Theory: Harvard University Press, 1464 pp.

Grad, M., and Tiira, T., 2009, The Moho depth map of the European Plate: Geophys. J. Int., **176**, 279–292.

Grad, M., and Tiira, T., 2012, Moho depth of the European Plate from teleseismic receiver functions: J. Seismology, **16**, 95–105.

Hafkenscheid, E., Wortel, M., and Spakman, W., 2006, Subduction history of the Tethyan region derived from seismic tomography and tectonic reconstructions: J. Geophys. Res., Solid Earth, **111**, B08401, doi: 10.1029/2005JB003791.

Hatzfeld, D., Tatar, M., Priestley, K., and Ghafory-Ashtiany, M., 2003, Seismological constraints on the crustal structure beneath the

Zagros Mountain belt (Iran): Geophys. J. Int., **155**, 403–410.

Kennedy, J., Kennedy, J. F., Eberhart, R. C., and Shi, Y., 2001, Swarm Intelligence: Morgan Kaufmann, 512 pp.

Liu, S., Hu, X., and Liu, T., 2014, A stochastic inversion method for potential field data: ant colony optimization: Pure and Applied Geophysics, **171**, 1531–1555.

Manaman, N. S., and Shomali, H., 2010, Upper mantle S-velocity structure and Moho depth variations across Zagros belt, Arabian–Eurasian plate boundary: Physics of the Earth and Planetary Interiors, **180**, 92–103.

Manaman, N. S., Shomali, H., and Koyi, H., 2011, New constraints on upper-mantle S-velocity structure and crustal thickness of the Iranian plateau using partitioned waveform inversion: Geophys. J. Int., **184**, 247–267.

Molinaro, M., Zeyen, H., and Laurencin, X., 2005, Lithospheric structure beneath the south-eastern Zagros Mountains, Iran: recent slab break-off?: Terra Nova, **17**, 1–6.

Monteiro Santos, F. A., 2010, Inversion of self-potential of idealized bodies' anomalies using particle swarm optimization: Computers & Geosciences, **36**, 1185–1190.

Motavalli-Anbaran, S.-H., Zeyen, H., and Ardestani, V. E., 2013, 3D joint inversion modeling of the lithospheric density structure based on gravity, geoid and topography data—Application to the Alborz Mountains (Iran) and South Caspian Basin region: Tectonophysics, **586**, 192–205.

Motavalli-Anbaran, S.-H., Zeyen, H., and Jamasb, A., 2016, 3D crustal and lithospheric model of the Arabia–Eurasia collision zone: J. Asian Earth Sciences, **122**, 158–167.

Motavalli-Anbaran, S. H., Zeyen, H., Brunet, M. F., and Ardestani, V. E., 2011, Crustal and lithospheric structure of the Alborz Mountains, Iran, and surrounding areas from integrated geophysical modeling: Tectonics, 30, TC5012, doi: 10.1029/2011TC002934.

Mutlu, A. K., and Karabulut, H., 2011, Anisotropic Pn tomography of Turkey and adjacent regions: Geophys. J. Int., **187**, 1743–1758.

Paul, A., Kaviani, A., Hatzfeld, D., Vergne, J., and Mokhtari, M., 2006, Seismological evidence for crustal-scale thrusting in the Zagros mountain belt (Iran): Geophys. J. Int., **166**, 227–237.

Pavlis, N. K., Holmes, S. A., Kenyon, S. C., and Factor, J. K., 2012, The development and evaluation of the Earth Gravitational Model 2008 (EGM2008): J. Geophys. Res., **117**, B04406, doi: 10.1029/2011JB008916.

Rao, C. V., Raju, M., and Chakravarthi, V., 1995, Gravity modelling of an interface above which the density contrast decreases hyperbolically with depth: J. Applied Geophys., **34**, 63–67.

Rao, D. B., 1990, Analysis of gravity anomalies of sedimentary basins by an asymmetrical trapezoidal model with quadratic density function: Geophysics, **55**, 226–231.

Sen, M. K., and Stoffa, P. L., 2013, Global Optimization Methods in Geophysical Inversion: Cambridge University Press, 302 pp.

Shaw, R., and Srivastava, S., 2007, Particle swarm optimization: A new tool to invert geophysical data: Geophysics, **72**, F75–F83.

Shi, Y., and Eberhart, R., 1998, A modified particle swarm optimizer: Evolutionary Computation Proceedings, IEEE World Congress on Computational Intelligence, The 1998 IEEE International Conference.

Silva, J. B., Santos, D. F., and Gomes, K. P., 2014, Fast gravity inversion of basement relief: Geophysics, **79**, G79–G91.

Srivastava, S., and Agarwal, B. N. P., 2010, Inversion of the amplitude of the two-dimensional analytic signal of the magnetic anomaly by the particle swarm optimization technique: Geophys. J. Int., **182**, 652–662.

Wessel, P., Smith, W. H., Scharroo, R., Luis, J., and Wobbe, F., 2013, Generic mapping tools: improved version released: Eos. Trans. AGU, **94**, 409–410.

Zeyen, H., and Pous, J., 1993, 3-D joint inversion of magnetic and gravimetric data with a priori information: Geophys. J. Int., **112**, 244–256.

Zhdanov, M. S., 2002, Geophysical Inverse Theory and Regularization Problems: Elsevier, 633 pp.